Hydrodynamic Forces due to Orbital Stokes 5th Order Waves on Subsea Pipelines Resting on Porous Seabed

Annelise Karreman

Dr Jeremy Leggoe
School of Mechanical and Chemical Engineering

W/Prof Liang Cheng
School of Civil and Resource Engineering

CEED Client: Woodside Energy Ltd

Abstract

Stability design of subsea pipelines requires an accurate prediction of the hydrodynamic forces induced by waves and currents. Typically, rectilinear motion is used to simulate near seabed waves, since the orbital particle paths in wind-generated waves flatten to ellipsoids with depth. Together with linear Airy wave theory, this simplification predicts symmetric hydrodynamic forces on forward and reverse half wave cycles. Computational Fluid Dynamics (CFD) modelling of orbital waves has shown a difference in the overall pipeline stability of up to 50% between half wave cycles. Further CFD modelling is proposed to investigate and validate these results, with consideration given to the effects of higher order wave theory, boundary layer overshoot profile and a porous seabed.

1. Introduction

Pipeline stability is of significant importance to the success of hydrocarbon developments and can contribute up to 30% of the capital expenditure for pipeline projects on the North West Shelf, due to the severe metocean and geotechnical conditions. To avoid lateral instability, heavy concrete weight coating or costly secondary stabilisation methods (Zeitoun et al. 2009) are often required. The current design methods use DNV-RP-F109 (DNV 2011). The applicability of the Recommended Practice is currently being investigated through experiments conducted in the O-Tube facility under the STABLEPipe JIP. This facility, like many of the experimental investigations previously conducted, models the near bed wave velocity as rectilinear. CFD results have indicated an asymmetry in horizontal and vertical loading due to orbital wave velocities that may require consideration in design (King 2011).

The hydrodynamic load experienced by the pipeline is part of the flow induced forces "caused by the relative motion between the pipe and surrounding water" (DetNorskeVeritas 2008). Morison's equation has traditionally been used to calculate the loads on the pipe. The submerged weight is then increased to ensure the resistance of the system avoids lateral displacement. Morison's equation gives the hydrodynamic forces on a stationary cylinder as

$$F_H(t) = F_D(t) + F_I(t) = \frac{1}{2}\rho C_D u(t)|u(t)| + \frac{\pi D^2}{4}\rho C_M a_H(t) \qquad F_V(t) = F_L(t) = \frac{1}{2}\rho C_L D u(t)^2$$

where $F_H(t)$ and $F_V(t)$ are the time dependent horizontal and vertical forces, $F_D(t)$, $F_I(t)$ and $F_L(t)$ are the time dependent drag, inertia and lift forces, C_D, $C_M$and C_L are the constant drag, inertia and lift coefficients and $u(t)$ and $a_H(t)$ are the horizontal velocity and acceleration of fluid particles respectively. Morison's equation doesn't accurately model the forces under oscillatory flow due to the development of a wake that is swept back over the pipe in succeeding half wave cycles (Hale, Lammert, & Jacobsen 1989). Use of time-dependent coefficients and near pipe velocity produces a significant improvement in the calculation of forces under oscillatory wave loads (Bryndum, Jacobsen, & Tsahalis 1992).

Existing understanding of hydrodynamic loading is based on field measurements, which traditionally have not been accurate enough to capture the vertical component of orbital motion and experiments, conducted using the carriage technique, and in u-tube and o-tube facilities that model only the horizontal velocities. CFD Analysis predicts that an asymmetry of up to 50% of the overall pipeline stability exists between the forward and reverse half wave cycles when the vertical component of orbital wave motion is introduced (King 2011). It was also highlighted that the simplification to rectilinear motion produced conservative results when an absolute lateral stability design method is used. This suggests improved efficiency could be obtained by considering orbital motion in design methods.

2. Computational Fluid Dynamics (CFD) Model

Use of the CFD package ANSYS Fluent 13.0 to solve the Reynold Averaged Navier-Stokes (RANS) equations, allows for the computation of fluid velocities, pressures, turbulence parameters and hydrodynamic loading on the pipe structure within the model domain. Based on the previous mesh verification work, the domain consists of a 200m x 40m fluid region above a 200m x 2m porous medium seabed region with a 1m diameter pipeline located at the horizontal centre of the fluid region with its base level with the top of the porous medium. There is no gap between seabed and pipe and the seabed curves upward toward the pipe to make a contact angle of 45° reducing the likelihood of scour below the pipeline.

The left and top boundaries of the fluid region have been modelled as velocity inlets, whilst the right boundary of the fluid region has been set to a pressure outlet. The left, right and bottom boundaries of the porous region have been set to symmetry and act as a free slip wall. The pipe has been given the Nikuradse roughness of concrete. The proposed mesh contains 80,128 cells, with cell sizes biased towards the boundary layers at the seabed and around the circumference of the pipe. The smallest cell height is 0.6mm which is sufficiently small to capture the boundary layer whilst keeping the cell height larger than the grain diameter in the porous medium.

The Shear Stress Transport (SST) k-ω turbulence closure model is adopted in the model as a result of the previous work comparing the available 2D closure models in ANSYS Fluent (King 2011).

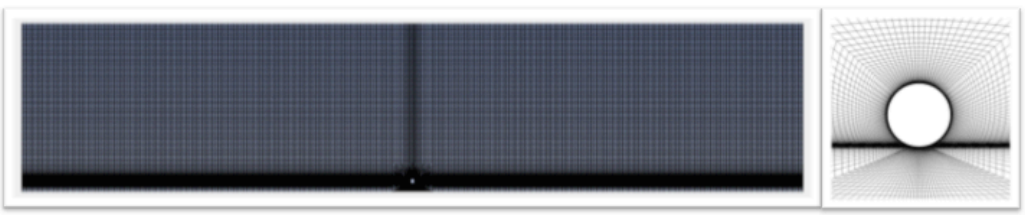

Figure 1 Mesh grids in computational domain (left). Mesh grid near pipe (right).

2.1 Porous Medium

ANSYS Fluent 13.0 allows for the modelling of porous medium as fluids with specified porosity, and viscous and inertial resistance coefficients. The ANSYS User's Guide (2011, Section 7.2.3) provides that the viscous resistance coefficient of a packed bed, $\frac{1}{\alpha}$, and the inertial resistance coefficient, C_2, can be calculated as

$$\alpha = \frac{D_p^2}{150}\frac{\epsilon^3}{(1-\epsilon)^2} \qquad C_2 = \frac{3.5}{D_p}\frac{(1-\epsilon)}{\epsilon^3}$$

where D_p is the particle diameter and ϵ is the void ratio. The soil parameters of the STABLEPipe JIP O-tube (An et al. 2012, p3) are used for the model.

The ANSYS User's Guide (2011, Section 7.2.3) provides warnings on the treatment of turbulence in the porous medium and suggests that unless large porosities are used the porous medium should be treated as a laminar region with zero turbulent viscosity, ν_t.

2.2 User Defined Function (UDF)

2.2.1 Specified Boundary Condition Profiles

The profiles for the horizontal and vertical component of the velocity and the values for the Turbulent Kinetic Energy (k) and Specific Dissipation Rate (ω) at the two velocity inlets, are defined using a User Defined Function (UDF). Considerable focus has been directed at refining the UDF interpreted into the model in ANSYS Fluent. The main UDF inputs are wave height (H), wave length (L), wave period (T) and water depth (d). The UDF specifies the profiles for the horizontal and vertical component of the velocity, and the values for the Turbulent Kinetic Energy (k) and Specific Dissipation Rate (ω) at the two velocity inlets. Reversed flow is permitted at the pressure outlet and the same profiles for k and ω are applied to this reversed flow.

Increased consistency in the model has been obtained by accurately specifying the k and ω profiles in the UDF. The chosen profiles are functions only of the height above the seabed and are transmitted through an equivalent empty domain without substantial changes occurring. Specifying these profiles in the UDF replicates the fully developed wave boundary layer.

2.2.2 Stokes 5th Order Wave Theory

A large number of the cases in the test matrix previously analysed (King 2001) lie in the applicability range of Stokes 5th order wave theory (See Figure 2). Although Airy wave theory has been found to provide "excellent predictions of near-bottom peak water velocities under waves" (Grace & Nicinski 1976, p684), higher order wave theories will provide improved prediction of seabed kinematics (Zeitoun et al. 2010, p1).

Stokes 5th order wave velocity profiles have been derived and are provided to the ANSYS Fluent model by interpreting the UDF. Stokes finite amplitude wave theory models the wave horizontal and vertical velocities as a Fourier series of the form

$$u = \sum_{n=1}^{5} a_n \cosh(n\frac{2\pi}{L}y)\cos\left(2\pi n(\frac{x}{L} - \frac{t}{T})\right) \qquad w = \sum_{n=1}^{5} a_n \sinh(n\frac{2\pi}{L}y)\sin\left(2\pi n(\frac{x}{L} - \frac{t}{T})\right)$$

where the a_n series of coefficients are calculated for the specific wave height, length, period and water depth of the wave in accordance with those proposed by Skjelbreia and Hendrickson (1961). Note that the CFD domain is chosen so as to avoid introducing the free-surface of the wave into the domain.

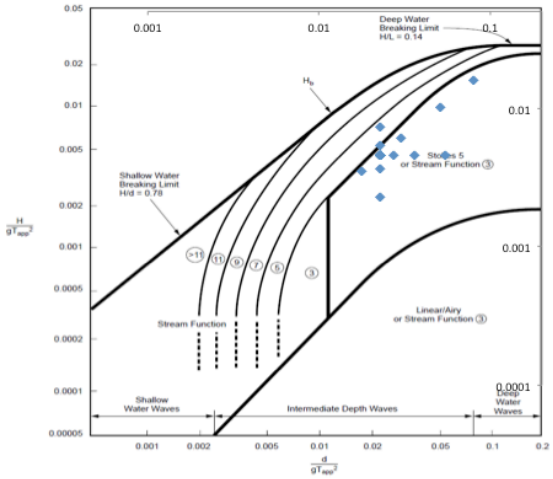

Figure 2 Wave theory applicability for test matrix (King 2011, p52).

The superposition of sinusoids produces a wave with a steeper crest and shallower trough than the basic sinusoidal function proposed by Airy wave theory. The horizontal and vertical velocity profiles are also slightly altered (see Figure 3). The introduction of Stokes 5th Order wave theory therefore introduces additional asymmetry into the hydrodynamics.

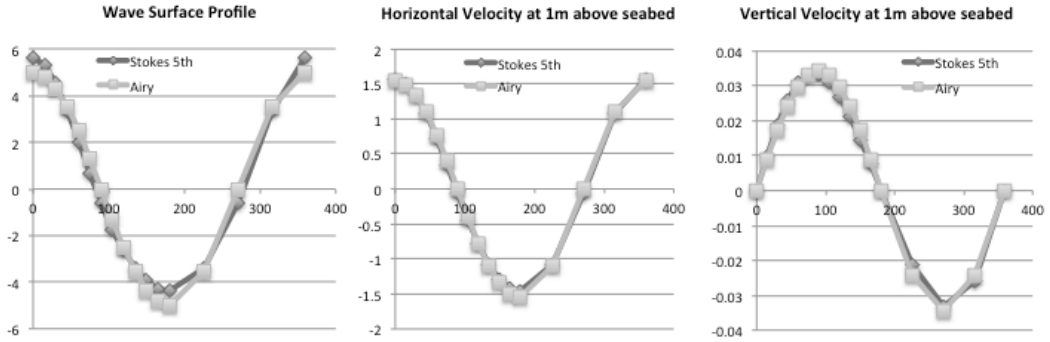

Figure 3 Wave Surface Profile (left), Horizontal Velocity at 1m above seabed (middle), Vertical Velocity at 1m above seabed (right) for the case 1 test matrix wave.

2.2.3 Wave Boundary Layer Velocity Profile

Boundary conditions in a wall boundary layer require the horizontal and vertical velocity to go to zero at the wall and reach the free stream velocity at the top of the boundary layer.

Lamb (1932) derived a continuous first order solution to the velocity profile in a laminar boundary layer by resolving the velocity as a cis function, where the velocity is given by the real part of $e^{i(kx-\omega t)}$, and introducing the concept of a defect velocity between the free stream

velocity and the boundary layer velocity with "the nature of a damped wave… propagat[ing] away from the bed" (Nielsen 1999, p16)

$$u = u_\infty \left(\cos\left(2\pi\left(\frac{x}{L} - \frac{t}{T}\right)\right) - e^{-\beta y}\cos\left(2\pi\left(\frac{x}{L} - \frac{t}{T}\right) - \beta y\right)\right)$$

where $\beta = \sqrt{\frac{\pi}{\upsilon T}}$ and υ is the kinematic viscosity of the fluid. This solution captures both the decay and phase difference in the velocity profile approaching a wall as seen in Figure 4.

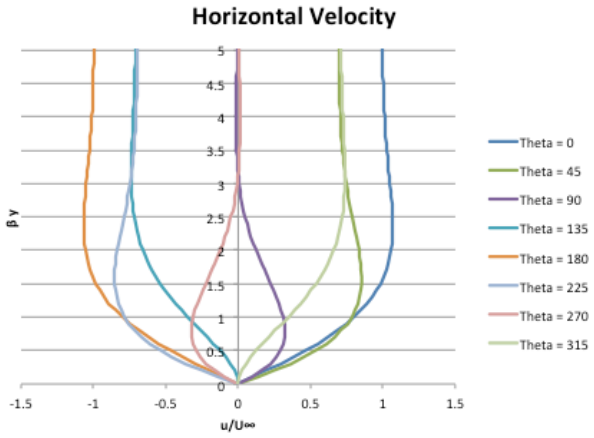

Figure 4 Boundary layer horizontal velocity profile.

The first order Lamb's solution is not appropriate for Stokes finite amplitude waves, since the velocity profile in the boundary layer is not symmetrical with respect to the vertical axis (Borghei 1982, p178-178). The profile used in the UDF has been derived through the same method as Lamb's solution.

Lamb's solution is also inaccurate in describing the velocity profile in transitional or turbulent flow (Nielsen 1992, p44). An alteration introducing a power law has been incorporated into the UDF.

The horizontal velocity profile of the UDF is given by

$$u = \sum_{n=1}^{5} a_n \cosh\left(n\frac{2\pi}{L}y\right)\left(\cos\left(2\pi n\left(\frac{x}{L} - \frac{t}{T}\right)\right) - e^{-\sqrt{n}\left(\frac{y}{z_{p1}}\right)^p}\cos\left(2\pi n\left(\frac{x}{L} - \frac{t}{T}\right) - \sqrt{n}\left(\frac{y}{z_{p2}}\right)^p\right)\right)$$

with z_{p1}, z_{p2} and p determined by optimising the fit of the function to the developed boundary layer velocity outputs from Fluent. The vertical velocity boundary layer (Svendsen 2006, p474-479), is not captured in the UDF.

3. Results and Discussion

Preliminary results have indicated the continuing presence of hydrodynamic loading asymmetry. The full test matrix has not been run and as such no reliable conclusions may yet be drawn.

4. Conclusions and Future Work

UDFs have been refined for a number of the original test matrix cases and it is proposed that these will be run through the improved mesh with porous seabed to verify and further quantify the identified asymmetry parameter. There is still scope for extension of the analysis to 3D CFD simulation to model the motion in the axial direction due to vortices.

5. References

An, H, Luo, C, Cheng, L & White, D, 2012, 'A Re-examination of the Hydrodynamic Forces acting on Partially-Buried Submarine Pipelines', *Proceedings of the thirty-first International Conference on Offshore Mechanics and Artic Engineering.*

ANSYS 2011, *ANSYS FLUENT 13.0 User's Guide*, ANSYS Inc.

Borghei, BM 1982, *Oscillatory boundary layer over fixed rough beds*, Ph.D. Thesis, University of Nottingham.

Bryndum, MB, Jacobsen, V & Tsahalis, DT 1992, 'Hydrodynamic Forces on Pipelines: Model Tests', *Journal of Offshore Mechanics and Arctic Engineering*, vol. 114, no. 4, pp. 231-241.

DetNorskeVeritas, 2008, *Offshore Standard DNV-OS-F101: Submarine Pipeline Systems*, DNV, Norway.

DNV 2011, *On-Bottom Stability Design of Submarine Pipelines*, vol. DNV-RP-F109, Det Norske Veritas, Norway.

Grace, RA & Nicinski, SA 1976, 'OTC2676: Wave Force Coefficients from Pipeline Research in the Ocean', *Proceedings of the eighth Offshore Technology Conference.*

Hale, JR, Lammert, WF & Jacobsen, V 1989, 'OTC6059: Improved Basis for Static Stability Analysis and Design of Marine Pipelines', *Proceedings of the twenty-first Offshore Technology Conference*.

King, L 2011, *Hydrodynamic Forces on Subsea Pipes due to Orbital Wave Effects*, Honours Thesis, University of Western Australia.

Lamb, 1932, *Hydrodynamics*, 6th Ed, Cambridge University Press.

Nielsen, P 1992, 'Coastal Bottom Boundary Layers and Sediment Transport', *Advanced Series in Ocean Engineering*, Vol 4.

Skjebreia, L & Hendrickson, J 1960, 'Fifth Order Gravity Wave Theory', 7th *Proceedings of the seventh International Conference of Coastal Engineering*, Chapter 10, pp. 184-196.

Svendsen I 2006, 'Introduction to nearshore hydrodynamics', *Advanced Series on Ocean Engineering*, Vol 24 World Scientific, Singapore.

Zeitoun, HO, Tornes, K, Cumming, G & Willcocks, J 2009, ' OMAE2009-79893 A Stability Design Rationale - A Review of Present Design Approaches', *Proceedings of the twenty-eighth International Conference on Offshore Mechanics and Artic Engineering.*